Review of confinement and transport studies in the TJ-II flexible heliac

2001 Nucl. Fusion 41 1449

(http://iopscience.iop.org/0029-5515/41/10/312)

Review of confinement and transport studies in the TJ-II flexible heliac

C. Alejaldre, L. Almoguera, J. Alonso, E. Ascasíbar, A. Baciero, R. Balbín, M. Blaumoser, J. Botija, B. Brañas, E. de la Cal, A. Cappa, R. Carrasco, F. Castejón, J. Castellano, J.R. Cepero, C. Cremy, J. Doncel, S. Eguilior, T. Estrada, A. Fernández, C. Fuentes, A. García, I. García-Cortés, J. Guasp, J. Herranz, C. Hidalgo, J.A. Jiménez, I. Kirpitchev, V. Krivenski, I. Labrador, F. Lapayese, K. Likin, M. Liniers, A. López-Fraguas, A. López-Sánchez, E. de la Luna, R. Martín, L. Martínez-Laso, K.J. McCarthy, F. Medina, M. Medrano, P. Méndez, B. van Milligen, M. Ochando, L. Pacios, I. Pastor, M.A. Pedrosa, A. de la Peña, A. Portas, J. Qin, L. Rodríguez-Rodrigo, J. Romero, A. Salas, E. Sánchez, J. Sánchez, F. Tabarés, D. Tafalla, V. Tribaldos, J. Vega, B. Zurro

Laboratorio Nacional de Fusión, Asociación Euratom–CIEMAT, Madrid, Spain

Abstract. TJ-II is a four period, low magnetic shear stellarator ($R = 1.5$ m, $a < 0.22$ m, $B_0 \leq 1.2$ T) which was designed to have a high degree of magnetic configuration flexibility. In the most recent experimental campaign, coupling of the full ECRH power ($P_{ECRH} \leq 600$ kW) to the plasma has been possible using two ECRH transmission lines which have different power densities. Both helium and hydrogen fuelled plasmas have been investigated. The article reviews the latest physics results in particle control, configuration effects, and transport and fluctuation studies.

1. Introduction

The TJ-II stellarator ($R = 1.5$ m, $a < 0.22$ m, $B_0 \leq 1.2$ T, $P_{ECRH} \leq 600$ kW, $P_{NBI} \leq 2$ MW currently being installed) has been operating in Madrid since 1998 [1]. TJ-II was designed to have a high degree of magnetic configuration flexibility, as is inherent to heliac devices. In addition, the rotational transform can be varied between 0.9 and 2.5, the magnetic well may be changed from -1% to 6%, and theory predicts maximum beta values as high as 6%.

The ECRH system of TJ-II consists of two gyrotrons operated at 53.2 GHz, the second harmonic of the electron cyclotron frequency in TJ-II plasmas. Each gyrotron can deliver up to 300 kW of microwave power at the output window for a pulse length of up to 1 s [2]. Two mirror lines transmit the microwave power from the gyrotrons to the plasma. The first transmission line (QTL1) has a fixed injection geometry, with a beam width at the plasma border of approximately 50 mm, and the power density is about 1 W/cm^3. The second transmission line (QTL2) incorporates a movable mirror located inside the vacuum vessel which permits experiments on central and off-axis heating, as well as on current drive, to be carried out. Its beam is focused at the plasma centre, its waist is about 9.5 mm and its power density is 25 W/cm^3. In the experiments reported in this article, coupling of the full ECRH power to the plasma has been possible using two ECRH transmission lines with different power densities (1 and 25 W/cm^3) and different launch steering capabilities (fixed versus poloidal and toroidal variation). Both helium and hydrogen fuelled plasmas have been investigated. At present, NBI injectors and ion sources are being installed on TJ-II [3, 4] and when these are operating, the plasma will be heated by two hydrogen beams, each with around 1 MW of power, mounted in a co–counter configuration. The NBI beam energy is 40 keV in order to optimize absorption, while the maximum pulse length is 300 ms. It is expected that the injectors will be ready for plasma heating in the second half of 2001. Finally, a state of the art set of plasma diagnostics is in operation [5] and a dedicated data acquisition system provides resources for remote participation and control [6].

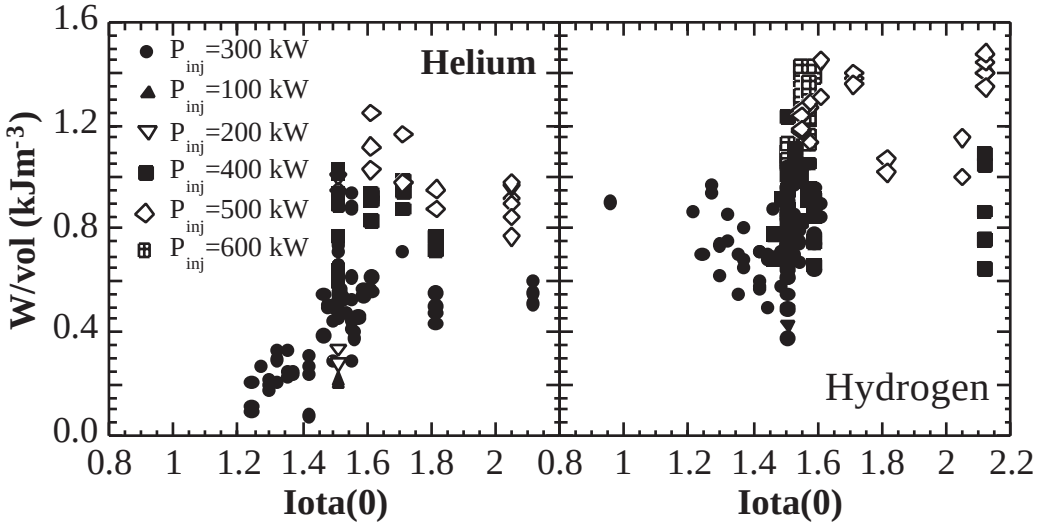

Figure 1. Evolution of diamagnetic energy content normalized to the calculated configuration volume as a function of rotational transform for helium and hydrogen plasmas and several values of heating power.

2. Particle control and wall conditioning

In order to achieve reproducible and controlled discharges for full ECRH power injection, new gas control and wall conditioning techniques have been implemented. This has required the sequential application of He (overnight) and Ar (<30 min) glow discharges to the metallic vessel and the development of a gas injection monitoring system for very low gas flows (<0.05 Pa m^3 s^{-1}) [7]. Low Z effective values and low radiated powers (<20%) are typically achieved for all plasma heating schemes applied. These facts are consistent with the spectroscopic observations (lack of metallic species) and low values of desorbed Ar [8]. A wall desorption rate proportional to total injected power has been observed, and this has limited the operation in He at $P < 600$ kW. This outgassing rate could not be attributed to the change in edge characteristics seen in density and power scans, and it suggests the occurrence of direct particle losses to the walls of the vacuum vessel.

3. Configurational effects

Magnetic configuration ($\iota \approx 1.28$–2.24) and plasma volume (0.6–1.1 m^3) scans have been investigated. Plasma stored energies (W) of up to 1.5 kJ have been measured for electron densities and temperatures of up to 1.2×10^{19} m^{-3} and 2.0 keV, respectively, with $P_{ECRH} \leq 600$ kW. The ion temperature is in the range 90–120 eV.

The dependence of the diamagnetic energy per unit plasma volume on the rotational transform has been studied for both helium and hydrogen plasmas. Although a positive iota dependence (in the low iota range) was reported for helium plasmas [9], recent results, which still have to be fully analysed, show no clear dependence of normalized energy content for hydrogen plasmas in the same iota region (Fig. 1). These latest discharges were made with the improved vacuum vessel conditions (additional Ar glow discharge cleaning) described in Ref. [10], thus the different behaviour found in helium and hydrogen plasmas might only indicate that the previous helium results correspond to discharges in which optimum confinement had not yet been reached. Obviously, further experiments are needed to elucidate this point.

Maximum chord averaged C V temperature and poloidal rotation data are plotted in Fig. 2 as a function of the central iota value. It can be seen that the lowest impurity temperature value corresponds to the lowest rotational transform and that, in this range, the shell where C V emission peaks rotates in the negative direction [11].

Thomson scattering measurements with high spatial resolution have revealed the presence of fine structures in both density and temperature profiles [12]. These structures consist of peaks and valleys

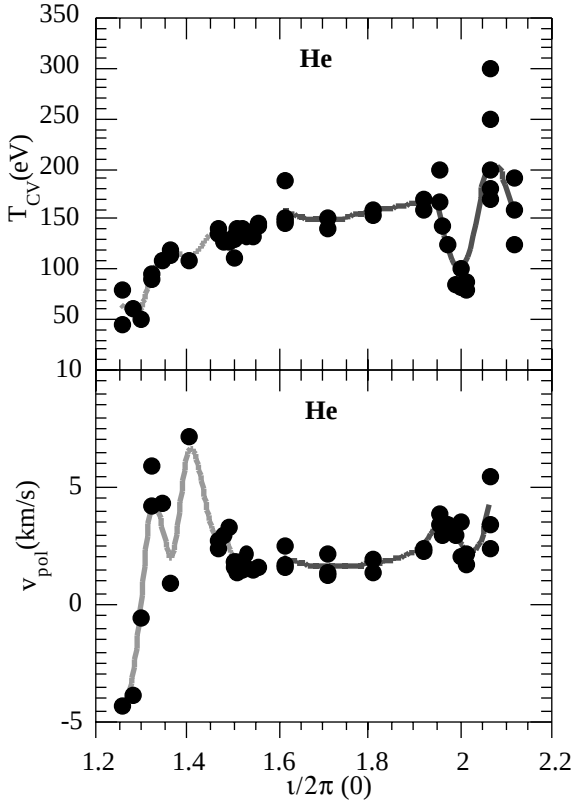

Figure 2. C V temperature and rotation versus iota.

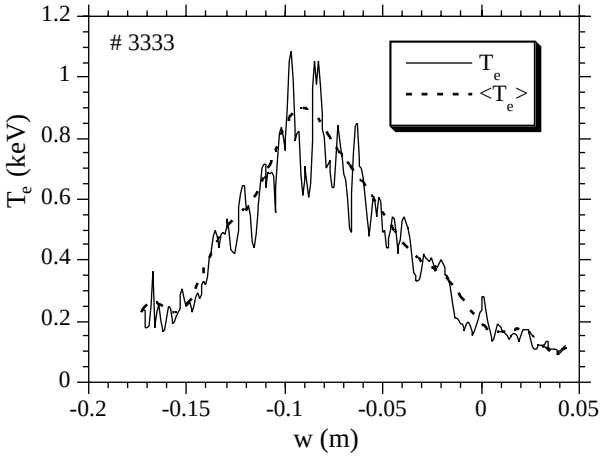

Figure 3. Typical Thomson scattering temperature profile along with the smoothed spline fit. The abscissa in this figure is a co-ordinate along the ruby laser passing through the plasma. Fine electron profile structures appear in all the discharges and configurations of TJ-II.

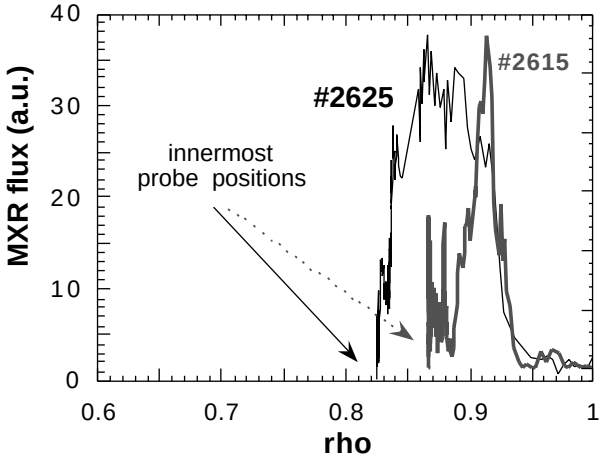

Figure 4. MXR flux from two discharges with the same magnetic configuration as a function of the effective radius.

superimposed on a smooth average (Fig. 3). Indeed, some irregularities remain in an ensemble average of discharges having similar macroscopic parameters such as line density, central temperature and plasma current. They have been found in plasmas heated by electron cyclotron waves for all magnetic configurations explored to date. Furthermore, studies of impurity radiation profiles using an automated pattern recognition procedure have also revealed the presence of topological structures [13]. Their possible link to the iota profile (i.e. rationals) is currently under investigation.

A special experimental set-up combining edge and X ray diagnostics has been used to locate fast electrons that are confined near singular magnetic surfaces at the plasma periphery [14]. Enhancements in bremsstrahlung emissions due to high energy electrons colliding with a fast reciprocating probe tip are related to the presence of relevant low order resonances. Figure 4 shows the intermediate energy (20–200 keV) X ray (MXR) flux measured for two shots with the same magnetic configuration. In shot 2625 no ECRH pulse was applied and therefore the emissions are due to runaway electrons. In shot 2615 a runaway electron suppressor acted before the 300 kW pulse (2 ms long) was applied [15] and the probe was inserted 80 ms after plasma extinction. As seen in the figure, the enhancement of the flux starts at the same radial location as that of the probe tip (expressed in terms of normalized effective radius), which according to theoretical calculations is close to the position of the $n/m = 8/5$ resonant surface. The present experiments show that, in the TJ-II stellarator, fast electrons ($E > 70$ keV) are confined in the vicinity of low order rational surfaces. Recent experiments have shown that rational surfaces located not only

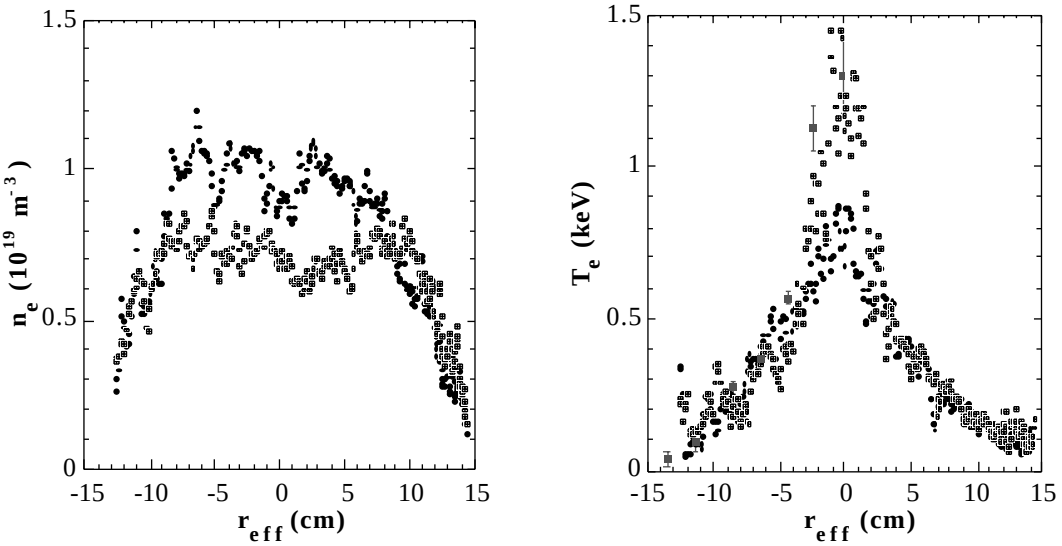

Figure 5. Thomson scattering profiles of helium plasmas with injected power of 300 kW, rotational transform $\iota(0) = 1.51$ and different electron density. The ECE temperature profile is displayed for the low density case in which an internal transport barrier appears.

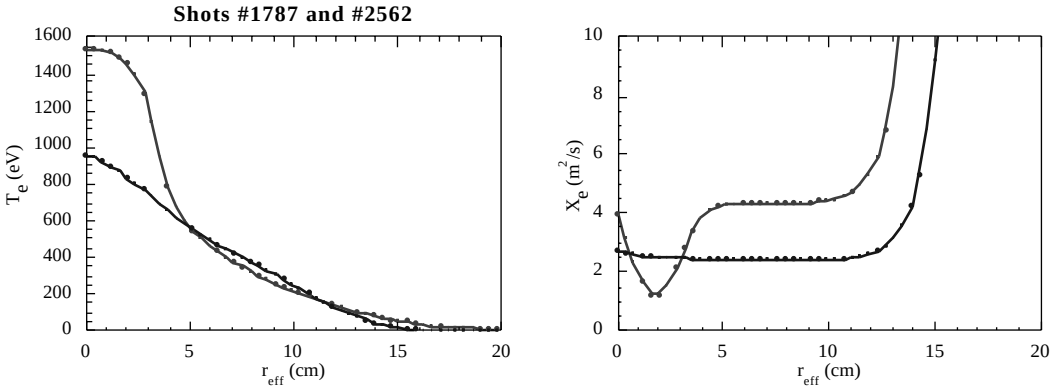

Figure 6. Transport analysis, obtained using the modified Proctr code, shows a reduction in transport coefficients in the presence of an internal transport barrier.

at the boundary but also deeper inside the plasma bulk may selectively confine electrons with appropriate energies [16].

4. Transport studies

Electron heat diffusivity has been investigated using ECRH power modulation experiments and power balance analysis. It has been found that the heat conductivity is about 4 m^2/s in the plasma core region and that it increases as the plasma boundary region is approached.

Electron temperature profiles measured using ECE and Thomson scattering diagnostics have shown evidence of internal heat transport barriers in the TJ-II stellarator [17] (Fig. 5). These features appear in the profiles when plasma heating is performed using the QTL2 ECRH transmission line. This line is characterized by a localized power deposition profile and a high power density. Transport analysis, obtained using a modified Proctr code, shows a reduction in transport coefficients (Fig. 6).

In a stellarator, the electron root may be established when a high electron flux is produced by EC

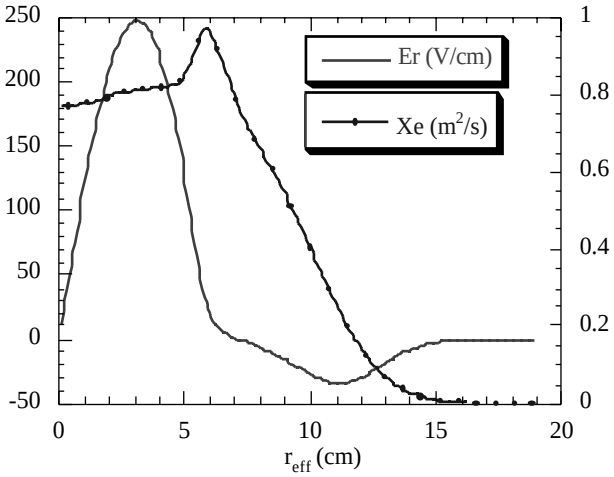

Figure 7. Neoclassical electric field and neoclassical conductivity calculated with a Monte Carlo code.

waves that push electrons to the ripple trapping region from where these particles can escape from the plasma. Then an ambipolar strong positive field, which improves the transport, is established. The neoclassical electric field and the neoclassical conductivity calculated with a Monte Carlo code [18] are plotted in Fig. 7.

Transport coefficients are close to neoclassical predictions derived from the Monte Carlo code for the transport barrier region. Ripple trapped electrons pumped out by ECRH and $\boldsymbol{E} \times \boldsymbol{B}$ decorrelation effects are candidates to explain these experimental results. Indeed, non-Maxwellian features have been observed in electron distribution functions in the 1–5 keV energy range, a finding which could be related to an ECRH induced deformation of the distribution function.

ELM-like activity has recently been observed in TJ-II [19]. These modes are observed in plasmas with relatively high electron densities and temperatures, i.e. in experiments with high ECRH power, $P \geq 300$ kW. Furthermore, the diamagnetic plasma energy content is typically greater than 1 kJ when an instability occurs. The appearance of a magnetic burst with frequency $f = 10$–30 kHz and amplitude $\tilde{B}_\theta/B \approx (2\text{–}3) \times 10^{-4}$ is accompanied by pronounced spikes in H_α emission and modulation of ECE signals in the plasma region where the temperature is in the range 100–200 eV (Fig. 8).

Transport analysis shows an important enhancement in electron thermal conductivity at the radial location of the ECE pivot point position. This would imply that the ELM-like instability modifies

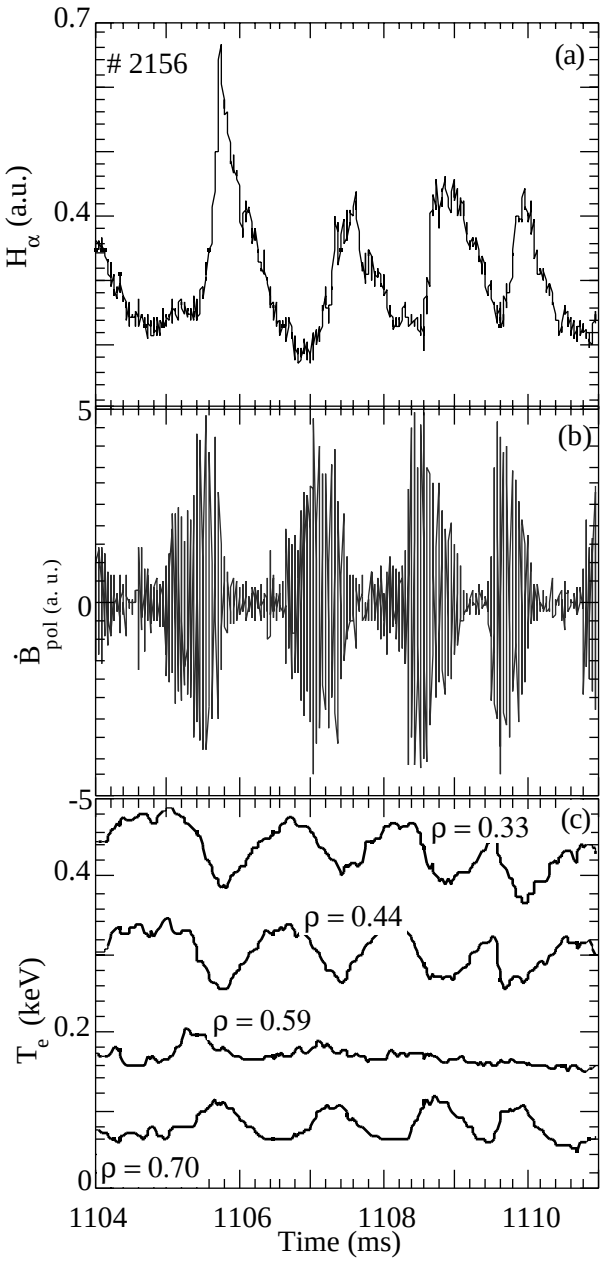

Figure 8. ELM-like MHD events in TJ-II.

transport properties in the region where it develops. The outward particle flux is enhanced while the plasma pressure gradient probably decreases, thereby producing the relaxation in the instability. The ELMs observed in tokamak plasmas produce a strong modification of the plasma profiles at the last closed flux surfaces (LCFSs), while in TJ-II this modification is observed a few centimetres inside the LCFS [19]. The nature of the MHD instability that triggers these modes is under study, but preliminary results show that an $m = 2$, $n = 3$ resonant

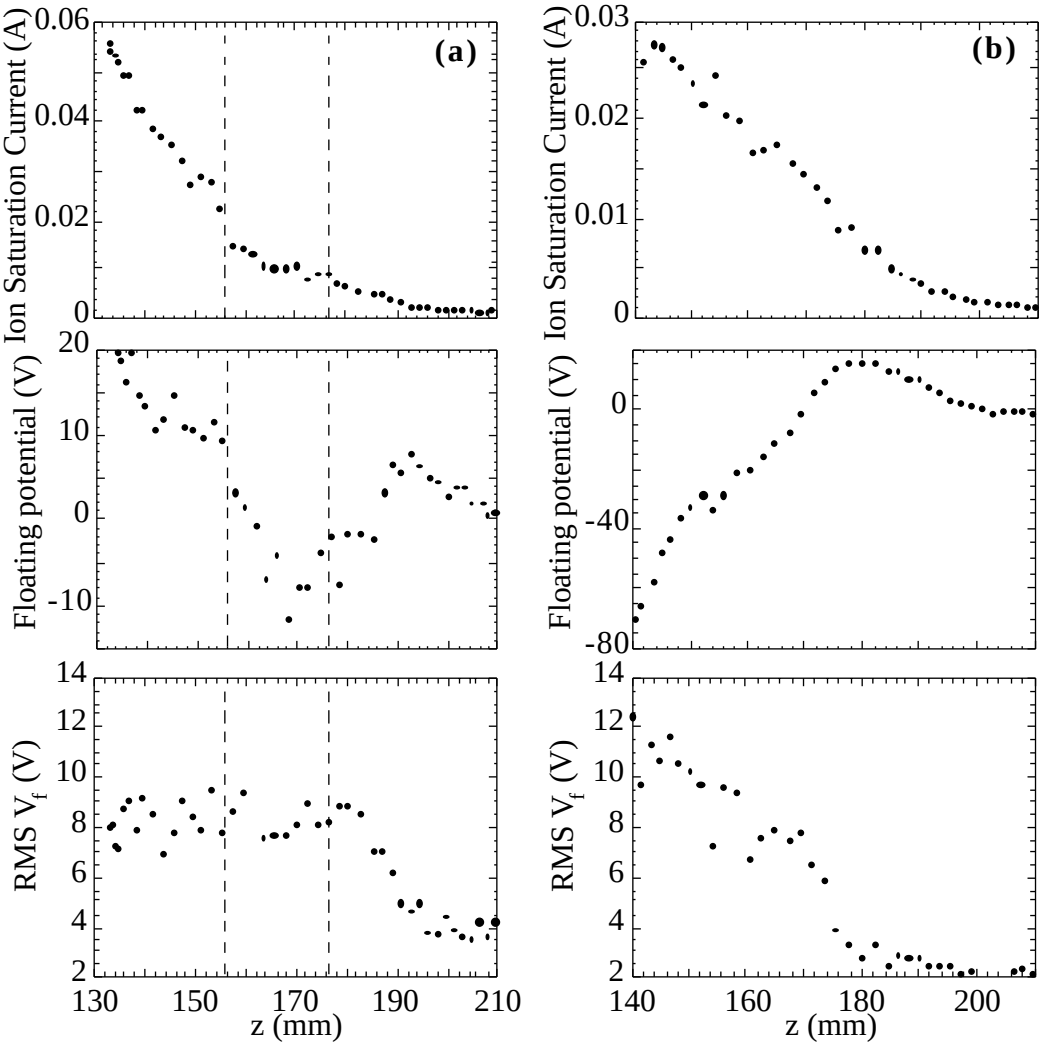

Figure 9. Radial profiles of the ion saturation current, floating potential and RMS of the floating potential measured (a) when the 4/2 rational surface was present in the plasma edge region and (b) when it was not.

mode interacting with a resistive ballooning instability located at the pivot point is the most probable cause for the event development observed. An analysis of plasmas in which these instabilities occur is under way and future work is necessary to clarify this point.

Edge parameters (electron density and temperature) have been investigated in both hydrogen and helium plasmas, for a fixed magnetic configuration, using He and Li atomic beams and Langmuir probes [20]. For this, density and power scans were carried out but no significant differences were detected between the hydrogen and helium plasmas. It has been found that edge characteristics are quite insensitive to operational parameters, as demonstrated by the constant edge densities for the central density scan and the constant edge temperatures for the power scan. However, a systematic broadening of edge profiles with P/n_e was seen. SOL particle e-folding lengths were also recorded. This allowed an evaluation to be made of diffusion coefficients and global particle confinement times under the assumption that no strong asymmetries exist. D values of the order of D_{Bohm}, and τ_p values ranging from 14 to 3 ms were also obtained. Finally, a clear degradation of particle confinement with injected power was found together with an indication of confinement enhancement with increased density.

5. Fluctuation studies

$\boldsymbol{E} \times \boldsymbol{B}$ sheared flows have been observed in the proximity of rational surfaces (8/5 and 4/2) of the plasma boundary region for different magnetic configurations [21, 22]. Frequency spectra are dominated by frequencies below 200 kHz with density fluctuation levels in the range 10–40%. A radial variation in the poloidal phase velocity of fluctuations has been observed near the 8/5 and 4/2 rational surfaces. The measured correlation time of fluctuations (10 μs) turns out to be comparable to the inverse of the $\boldsymbol{E} \times \boldsymbol{B}$ decorrelation rate, therefore suggesting a possible role of rational surfaces in accessing high confinement regimes. The TJ-II results (Fig. 9) look very similar to recent experiments carried out in the JET tokamak which showed a flattening in plasma profiles and evidence of $\boldsymbol{E} \times \boldsymbol{B}$ sheared flows linked to rational surfaces [23]. This similarity suggests that, in both tokamaks and stellarators, $\boldsymbol{E} \times \boldsymbol{B}$ sheared flows are linked to magnetic topology (rationals). Turbulence (via Reynolds stress), breakdown of ambipolarity and the presence of non-thermal electrons are all candidates for explaining the generation of $\boldsymbol{E} \times \boldsymbol{B}$ flows near resonant surfaces.

The flexibility of TJ-II allows its magnetic well depth to be modified over a broad range of values (0–6%). This high degree of flexibility makes it attractive for investigating transport characteristics close to instability thresholds. Indeed, radial profiles of ion saturation current and floating potential, as well as their fluctuations, have been obtained for magnetic configurations having the same rotational transform ($\iota(a) \approx 1.8$) but with the magnetic well varied from 0.2% to 2%. It has been found that the level of fluctuations increases for plasma configurations with the magnetic hill at the plasma edge (Fig. 10). This increase in fluctuation level is due to fluctuations in the frequency range (1–30 kHz). Interestingly, the breaking point in the frequency spectra (i.e. the $1/f$ region) is directly related to the level of fluctuations. Finally, these experimental results show the important role of the magnetic well in stabilizing pressure gradient instabilities in the TJ-II stellarator and open the possibility for investigating the properties of turbulent transport in the proximity of instability thresholds.

Measurement of wavenumber spectra is difficult in fusion devices owing to the fact that spatially resolved information is required. A comparative study of wavenumber spectra obtained using the high resolution Thomson scattering system (core plasma region) and Langmuir probes (edge region) is under way. To date (radial) wavenumber spectra show a remarkable similarity in shape. This does not appear to depend significantly on the measuring technique, the plasma region or plasma conditions. Specifically, wavenumber spectra obtained with the Thomson scattering system are similar to wavenumber spectra obtained with various other devices based on differing techniques [24]. The amplitude

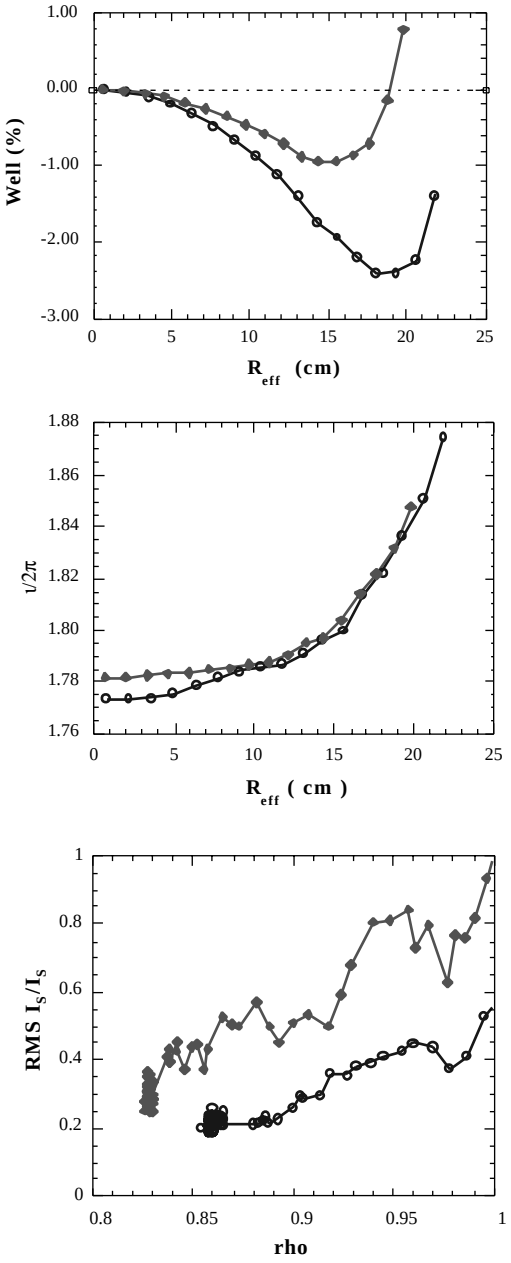

Figure 10. Magnetic well scan and fluctuations. The level of edge fluctuations increases in the plasma configuration with a magnetic hill in the plasma edge.

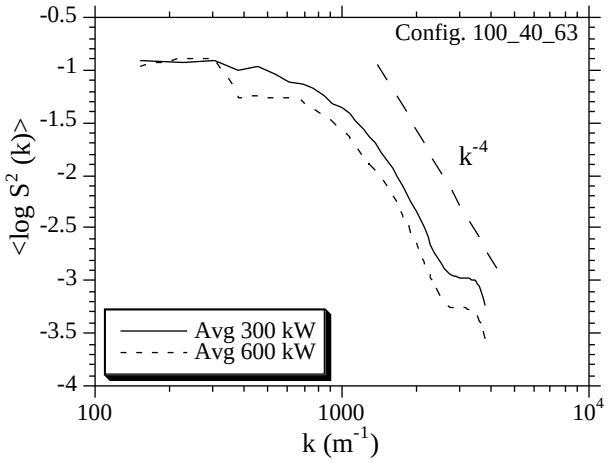

Figure 11. Spectrum of Thomson profiles as a function of heating power. Average over 33 discharges (300 kW) and 18 discharges (600 kW).

scales inversely with collisionality, but the shape is independent of plasma configuration (well, iota), global plasma parameters (temperature, density), and radial position (centre, edge). The spectral shape is characterized by a 'knee' at k = 5–10 cm^{-1} and a k^{-4}-like decay at large k (Fig. 11). Self-similarity analysis reveals the existence of a high degree of self-organization dominated by structures of about 2.5 cm in size. Various hypotheses exist to explain the nature of these fluctuations, for instance (a) magnetic islands (natural or otherwise), (b) kinetic effects related to ECRH, (c) 'filaments' and (d) broadband turbulence. A combination of several of these effects may be needed to reach a complete and satisfactory understanding of the observed structures.

6. Conclusions

It has been demonstrated that the flexibility of the TJ-II device is a powerful tool for physics studies in fusion plasmas. Coupling of the full ECRH power ($P_{ECRH} \leq 600$ kW) to the plasma has been possible using two ECRH transmission lines with different power densities. The important role played by magnetic topology (rational surfaces) in transport may be understood in terms of the competition between fluctuation induced transport mechanisms (which would degrade confinement) and $\boldsymbol{E}\times\boldsymbol{B}$ sheared flow mechanisms linked to rational surfaces. When $\boldsymbol{E}\times\boldsymbol{B}$ sheared flows reach a critical value, a spontaneous transport barrier may be formed near rational surfaces. Its magnetic well, which is the stabilizing mechanism in heliacs, makes TJ-II an ideal device for making a controlled study of the onset of turbulence and other related phenomena which are associated with the growth of instabilities. For the moment, however, no clear dependence of confinement on iota has been found.

In TJ-II, internal heat transport barriers appear in low density and high ECRH power density plasmas. ELM-like transport events increase heat conductivity. Such events can be triggered by a low order rational surface interacting with a resistive ballooning. Fine electron profile structures appear in all TJ-II discharges and configurations. This phenomenon may be due to broadband turbulence, which is enhanced by ECRH. The relationship with magnetic topology is under study.

References

[1] Alejaldre, C., et al., Plasma Phys. Control. Fusion **41** (1999) B109.
[2] Martin, R., et al., Fusion Technol. **1** (1998) 403.
[3] Liniers, M., et al., Fusion Technol. **1** (1998) 307.
[4] Guasp, J., et al., Fusion Technol. **35** (1999) 32.
[5] Sánchez, J., et al., J. Plasma Fusion Res. SERIES **1** (1998) 338.
[6] Vega, J., et al., Fusion Eng. Des. **43** (1999) 309.
[7] Tabares, F.L., et al., J. Nucl. Mater. **266–269** (1999) 1273.
[8] McCarthy, K.J., et al., in Controlled Fusion and Plasma Physics (Proc. 27th Eur. Conf. Budapest, 2000), Vol. 24B, European Physical Society, Geneva (2001) CD-ROM.
[9] Ascasíbar, E., et al., ibid.
[10] Tafalla, D., et al., in Proc. 14th Int. Conf. on Plasma Surface Interactions, Rosenheim, 2000.
[11] Zurro, B., et al., in Controlled Fusion and Plasma Physics (Proc. 27th Eur. Conf. Budapest, 2000), Vol. 24B, European Physical Society, Geneva (2001) CD-ROM.
[12] Herranz, J., et al., Phys. Rev. Lett. **85** (2000) 4715.
[13] Baciero, A., et al., in Controlled Fusion and Plasma Physics (Proc. 27th Eur. Conf. Budapest, 2000), Vol. 24B, European Physical Society, Geneva (2001) CD-ROM.
[14] Ochando, M.A., et al., in Proc. 12th IAEA Stellarator Workshop, Madison, 1999.
[15] Rodríguez-Rodrigo, L., et al., in Controlled Fusion and Plasma Physics (Proc. 26th Eur. Conf. Maastricht, 1999), Vol. 23J, European Physical Society, Geneva (1999) 353.
[16] Medina, F., et al., Rev. Sci. Instrum. (in press).
[17] Castejon, F., et al., in preparation.

[18] Tribaldos, V., et al., in Controlled Fusion and Plasma Physics (Proc. 26th Eur. Conf. Maastricht, 1999), Vol. 23J, European Physical Society, Geneva (1999) 349.
[19] García-Cortés, I., et al., Nucl. Fusion **40** (2000) 1867.
[20] Tabares, F.L., et al., in Controlled Fusion and Plasma Physics (Proc. 27th Eur. Conf. Budapest, 2000), Vol. 24B, European Physical Society, Geneva (2001) CD-ROM.
[21] Hidalgo, C., et al., Plasma Phys. Control. Fusion **42** (2000) A153.
[22] Pedrosa, M.A., et al., in Controlled Fusion and Plasma Physics (Proc. 27th Eur. Conf. Budapest, 2000), Vol. 24B, European Physical Society, Geneva (2001) CD-ROM.
[23] Hidalgo, C., et al., in preparation.
[24] Van Milligen, B.P., et al., Nucl. Fusion **41** (1991) 447.

(Manuscript received 9 October 2000
Final manuscript accepted 11 January 2001)

E-mail address of C. Alejaldre:
carlos.alejaldre@ciemat.es

Subject classification: F1, Se; B0, Se